Nanoscale Morphology of Polyanhydride Copolymers

Matt J. Kipper,[†] Sheng-Shu Hou,[‡] Soenke Seifert,[§] P. Thiyagarajan,[⊥] Klaus Schmidt-Rohr,[‡] and Balaji Narasimhan*,[†]

Department of Chemical and Biological Engineering, Iowa State University, Ames, Iowa 50011-2230; Department of Chemistry, Iowa State University, Ames, Iowa 50011; Advanced Photon Source, Argonne National Laboratory, 9700 S. Cass Avenue, Argonne, Illinois 60439; and Intense Pulsed Neutron Source, Argonne National Laboratory, 9700 S. Cass Avenue, Argonne, Illinois 60439

Received June 16, 2005; Revised Manuscript Received August 10, 2005

ABSTRACT: The microphase separation in polyanhydride random copolymers composed of 1,6-bis(*p*-carboxyphenoxy)hexane and sebacic acid is described. Though the copolymers are random, the monomers are sufficiently long and the segment−segment interaction parameter is sufficiently high to promote microphase separation when the copolymer is rich in one component. Solid-state NMR spin diffusion experiments and synchrotron small-angle X-ray scattering are used to discern the length scales of the microphase separation. Both techniques reveal a nanostructure with domain sizes less than 25 Å. This nanostructure is compared to approximate calculations of chain dimensions based on a random coil model and discussed in the context of the rational design of these materials for drug delivery applications.

Introduction

Polyanhydrides are a class of surface-erodible polymers that have been investigated as potential vehicles for drug delivery and other biomedical applications.[1−6] The erosion kinetics of polyanhydride copolymers can be modulated by altering the copolymer composition, when the two constituent polymers have different erosion rates.[6,7] This strategy has proven effective for controlled release applications. In our previous work, we have demonstrated that some polyanhydride copolymers exhibit microphase separation and that this microphase separation affects the mechanism of erosion and drug release kinetics when the relative erosion rates of the two constituent phases are different.[7−11] The rational design of controlled release formulations requires a detailed description of polymer microstructure in order to predict drug release kinetics.

We have focused on copolymers based on 1,6-bis(*p*-carboxyphenoxy)hexane (CPH) and sebacic acid (SA). These monomers are shown in Figure 1. Previously, we have described the crystallinity and crystallization kinetics of these copolymers by wide-angle X-ray scattering (WAXS), differential scanning calorimetry (DSC), and small-angle X-ray scattering (SAXS).[8,12] We have quantitatively studied the phase behavior of the poly(CPH)/poly(SA) blend system by SAXS, atomic force microscopy (AFM), optical microscopy, and molecular simulations in order to determine the segmental interaction parameter (χ) as a function of temperature.[13] This is shown in eq 1.

$$\chi = -2.04 + \frac{802}{T} \tag{1}$$

Here T is in K. We have also qualitatively described the microphase separation in CPH:SA copolymers by AFM and demonstrated its effects on drug release kinetics.[7,9,11]

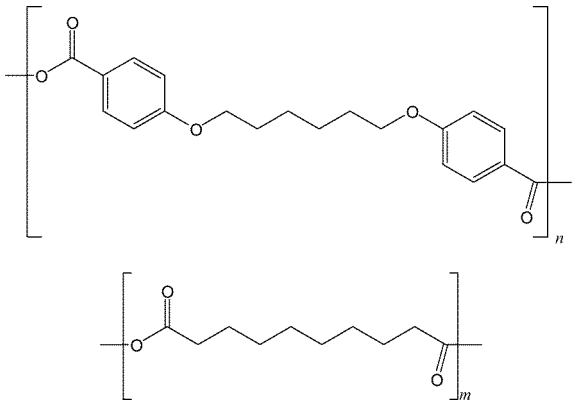

Figure 1. CPH monomer (top) and SA monomer (bottom).

We note that the copolymers described in this study are random copolymers, with reactivity ratios close to unity.[14] Thus, copolymer compositions rich in one monomer, for instance, SA, will contain more SA−SA bonds than SA−CPH or CPH−CPH bonds. Additionally, because the monomers have different hydrophobicity, the copolymers, when containing one type of monomer in excess, exhibit microphase separation.

The molecular architecture has been previously studied by ^{1}H NMR.[7,14,15] Since the monomer units are sufficiently long, and the segment−segment interaction parameter is sufficiently high, even relatively short sequence lengths (<15) promote microphase separation at the nanometer length scale. Thus, we refer to these copolymers as "weakly segregated, blocklike copolymers". Not all compositions of these copolymers exhibit such behavior. The melt polycondensation route used here for the synthesis of the polymers results in high polydispersity in chain length and presumably in sequence length. Thus, copolymer compositions containing nearly equal amounts of the two constituent monomers (e.g., poly(CPH:SA) (50:50)) do not demonstrate mi-

[†] Department of Chemical and Biological Engineering, Iowa State University.
[‡] Department of Chemistry, Iowa State University.
[§] Advanced Photon Source, Argonne National Laboratory.
[⊥] Intense Pulsed Neutron Source, Argonne National Laboratory.
* Corresponding author: e-mail nbalaji@iastate.edu, Tel (515) 294-8019, Fax (515) 294-2689.

10.1021/ma051267r CCC: $30.25
Published on Web 09/09/2005

crophase separation. However, compositions relatively rich in one component (e.g., poly(CPH:SA) (80:20) and poly(CPH:SA) (20:80)) have molecular architectures characterized by relatively long segments (10−15) of the majority monomer punctuated by short sequences (2−4) of the minority monomer.[7] A sequence of 10 SA monomers contains 110 backbone bonds, and a sequence of 10 CPH monomers contains 190 backbone bonds.

Our hypothesis of the microphase separation is predicated upon detailed studies of the erosion and drug release kinetics from these copolymers and upon characterization of the copolymer microstructure by atomic force microscopy[7,9] and solution NMR. In these studies we noted that as the polymer degrades, the two monomers are not released at the same rate. Additionally, in drug-loaded copolymers, the drug release kinetics is highly correlated to one of the individual monomer release profiles, depending on the monomer−drug compatibility. We concluded from these observations that the copolymers have a microphase-separated structure that permits partitioning of the drug between the two phases. We have successfully modeled the erosion and drug release kinetics by assuming a microphase-separated structure, but we have not described the structure in detail.[10,11] We further hypothesize that the microphase-separated domains are very small—on the order of a few nanometers in size—based on the average sequence lengths. In the current study, we use two experimental techniques that provide nanometer length scale resolution, solid-state NMR, and small-angle X-ray scattering (SAXS) to explore the morphology of these blocklike copolymers. Previously, McCann et al.[16] and Heatley et al.[15] have used solid-state NMR to investigate the relative degradation rates of the constituent monomers of a similar polyanhydride copolymer system; however, to our knowledge, the work presented here provides the first direct experimental evidence of the microphase separation in these copolymers.

Experimental Section

Polymer Synthesis and Characterization. Details of the polymer synthesis and characterization are reported elsewhere.[12] The poly(CPH:SA) (20:80) has an M_n of 9600 and a polydispersity index (PDI) of 2.2. The poly(CPH:SA) (80:20) has an M_n of 9700 and a PDI of 2.1. The degrees of polymerization are 45 and 31 for the 20:80 and 80:20 copolymers, respectively. ^{1}H NMR of the copolymers revealed that the actual compositions were 17:83 and 78:22, but we refer to them here by their nominal compositions, 20:80 and 80:20, respectively. The homopolymers were also synthesized and characterized as controls. The characterization of these materials is also reported elsewhere.[12]

Solid-State NMR. Solid-state NMR spin diffusion experiments for probing microphase separation in copolymers are conducted by first establishing a ^{1}H magnetization gradient that is based on some difference between the characteristic spectra of the two phases. Next a series of spectra at different mixing times, t_m, are taken that permits observation of the return to a homogeneous distribution of magnetization. In our experiments a chemical shift filter is used to suppress the magnetization of the aliphatic protons, thus removing all magnetization in the SA monomers.[17,18] Magnetization of the aromatic protons in the CPH monomers is passed to the aliphatic protons via ^{1}H "spin diffusion". After cross-polarization from ^{1}H to ^{13}C, the magnetization level in the various segments is detected with the superior site resolution of ^{13}C NMR with TOSS (total suppression of sidebands). The kinetics of spin diffusion reveals the characteristic length scale of the microstructure. Specifically, the time, t_m^s, required to reach equilibrium in the initial-rate regime is related to the domain size by[18,19]

$$d_{A,NMR} = \frac{\epsilon}{f_B'}\sqrt{4Dt_m^s/\pi} \quad (2)$$

Here, $d_{A,NMR}$ is the characteristic diameter of the minority (dispersed) phase A, f_B' is the fraction of the matrix phase B, D is the spin diffusion coefficient, and ϵ is a "dimensionality" parameter determined by the geometry. In this study, cylindrical domains are assumed ($\epsilon = 2$). The most reliable domain size information is obtained by going beyond the initial-rate analysis of eq 2 and simulating the full spin diffusion curve, for instance by calculating the magnetization evolution of protons on a lattice using the discretized form of the diffusion equation.[19] The $d_{A,NMR}$ in eq 2 is the diameter of the dispersed phase. The spacing between the dispersed domains can then be calculated from the estimated volume fractions of the two constituent phases and knowledge of the geometry (i.e., cylindrical domains).

Small-Angle X-ray Scattering (SAXS). Samples were prepared for SAXS by melting the polymer into DSC aluminum sample pans (Perkin-Elmer, Shelton, CT). As we have reported previously,[12] these make ideal sample holders because the aluminum is fairly transparent to the high-energy X-rays used in this study, and they allow us to use the DSC to control the thermal history of the samples prior to the SAXS experiments. The thickness of each sample was accurately determined using a micrometer and the values were between 700 and 800 μm. Prior to the SAXS measurement, the samples were annealed in a DSC (DSC7, Perkin-Elmer) by heating above the melting temperature for 5 min and then rapidly quenched to below the T_g. The SAXS experiments were conducted at Beamline 12-ID at the synchrotron beam source at Argonne National Laboratory.[20] The incident beam energy was 12 keV ($\lambda = 1.035$ Å). A 15 cm × 15 cm CCD detector, at a distance of 0.805 m from the sample, was used to measure the scattering data, and the transmitted beam intensity was measured using a photodiode on the beam stop. The scattering data were appropriately corrected and azimuthally averaged to obtain the one-dimensional intensity data, $I(q)$, as a function of scattering vector, q ($q = 4\pi \sin(\theta/2)/\lambda$; θ = scattering angle; λ = incident radiation wavelength). Five sets of data were collected and averaged for each sample. The resulting data were corrected for the scattering from the blank aluminum sample pan.

Results and Discussion

Solid-State NMR. A series of ^{13}C NMR spectra as a function of the ^{1}H spin diffusion time, t_m, are shown in Figure 2 for the poly(CPH:SA) (80:20) and (20:80). In (a), transfer of magnetization from the aromatic rings in CPH, selected by the chemical shift filter, to the aliphatic sites is clearly seen. In poly(CPH:SA) (20:80), signals of crystalline SA prevented us from observing the broader SA signals in the noncrystalline regions of interest. Therefore, we suppressed the ^{13}C signals of rigid (i.e., crystalline) CH_n groups by dipolar dephasing (gated decoupling) of 40 μs before detection. The signals of the partially mobile noncrystalline aliphatic segments with their reduced C−H dipolar couplings are retained. As a result of the double filtering, the signal-to-noise ratio in the poly(CPH:SA) (20:80) spectra is significantly reduced.

The peak intensity at 34 ppm representing aliphatic sites in the SA is used to analyze the spin diffusion quantitatively. After correction for the T_1 relaxation during t_m, the normalized intensities as a function of mixing time (t_m) are plotted in Figure 3, along with a fit obtained using a spin diffusion coefficient of 0.15 nm^2/ms. This is lower than the value of 0.8 nm^2/ms deter-

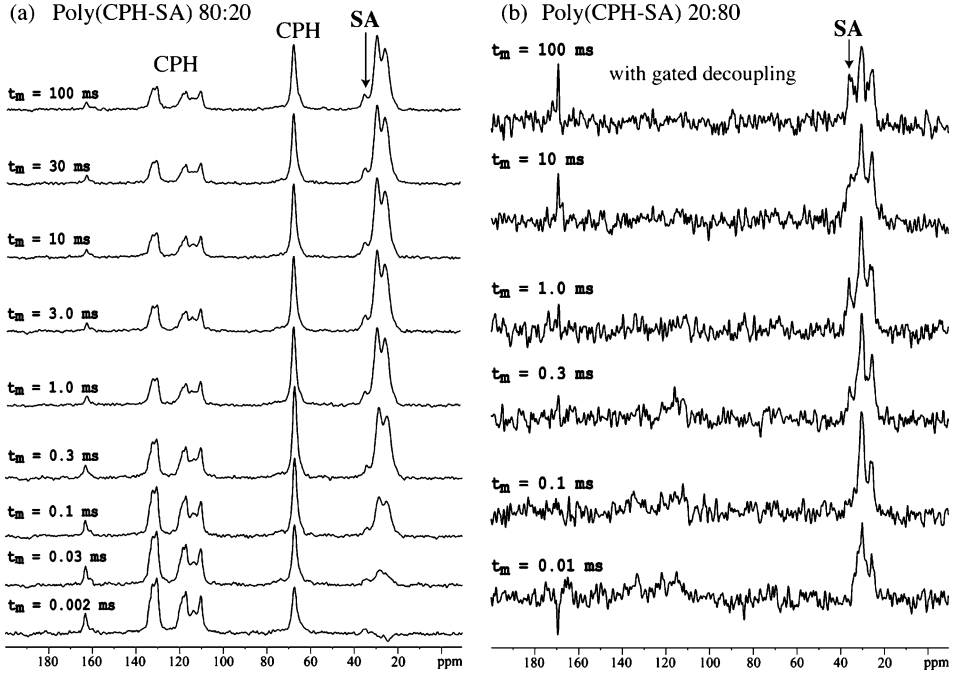

Figure 2. Series of ^{13}C NMR spectra after aromatic proton selection and ^1H spin diffusion times (t_m) as indicated: (a) poly(CPH:SA) (80:20), (b) poly(CPH:SA) (20:80). Gated decoupling (dipolar dephasing) of 40 μs was applied before detection in (b).

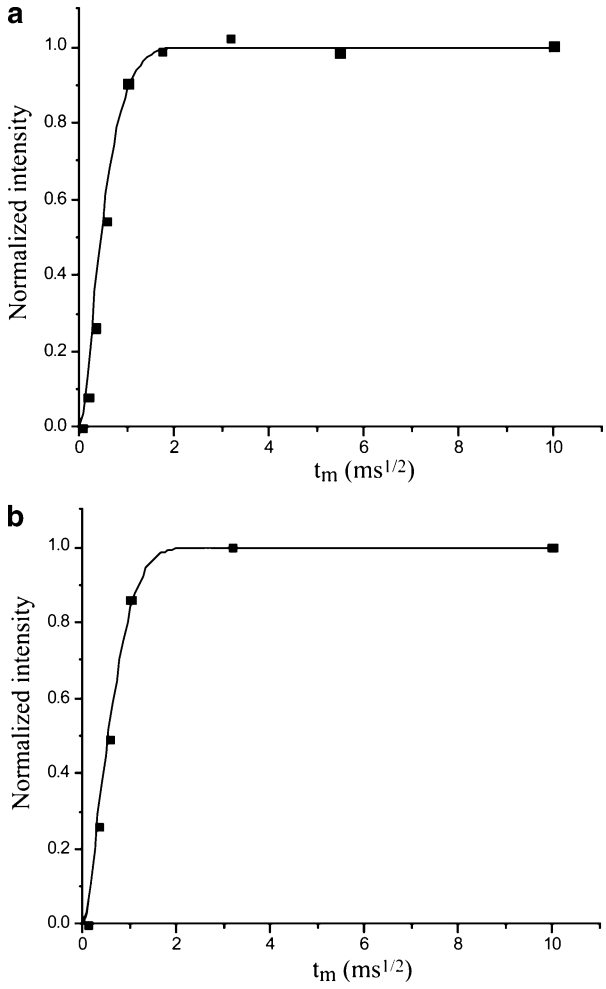

Figure 3. Normalized intensities at 34 ppm from spin diffusion spectra in Figure 2: (a) poly(CPH:SA) (80:20) and (b) poly(CPH:SA) (20:80). The line represents the fit of a diffusion model[18] to the data.

Table 1. Domain Sizes Obtained from Solid-State NMR[a] and SAXS

polymer	$d_{CPH,NMR}$ (Å)	$d_{SA,NMR}$ (Å)	$d_{CPH,SAXS}$ (Å)	$d_{SA,SAXS}$ (Å)
poly(CPH:SA) (20:80)	11[b]	(10)	10.0	
poly(CPH:SA) (80:20)	(14)	7[b]		9.1

[a] The numbers in parentheses represent the "domain size" of the majority (i.e., matrix) component. They have been calculated from the measured diameters of the minority (i.e., dispersed) phase and the volume fractions of the two phases. [b] The uncertainty in the measurement is ±4 Å.

mined on the 10 nm scale in rigid block copolymers[18] because we have found that on the 1 nm scale D values of ~0.25 nm^2/ms are more appropriate.[21] Furthermore, it takes into account some motional averaging of $^1H-^1H$ couplings due to the mobility in the noncrystalline aliphatic segments. Use of this relatively low D value also prevents us from overestimating the domain sizes. Note that the length scales derived from the data do not depend linearly on D, but only on $D^{1/2}$. Assuming cylindrical domains ($\epsilon = 2$), we obtain the characteristic "domain" diameters shown in Table 1. The main uncertainty in the measurement arises from the diffusion coefficient, and the unknown or assumed geometry and is ±4 Å.

SAXS. The SAXS data in the region of interest, shown in Figure 4, exhibit a sharp peak corresponding to the domain size of the minority component. The domain size is calculated from

$$d = \frac{2\pi}{q^*} \tag{3}$$

Here, q^* is the position of the peak. The domain size from the SAXS profiles is also given in Table 1. This sharp peak appears at a much higher q than the peak positions associated with the crystallinity,[12] which occur at $q < 0.05$ $Å^{-1}$. The lack of higher order reflections indicates that there is no correlated periodic structure and is consistent with the aforementioned polydispersity

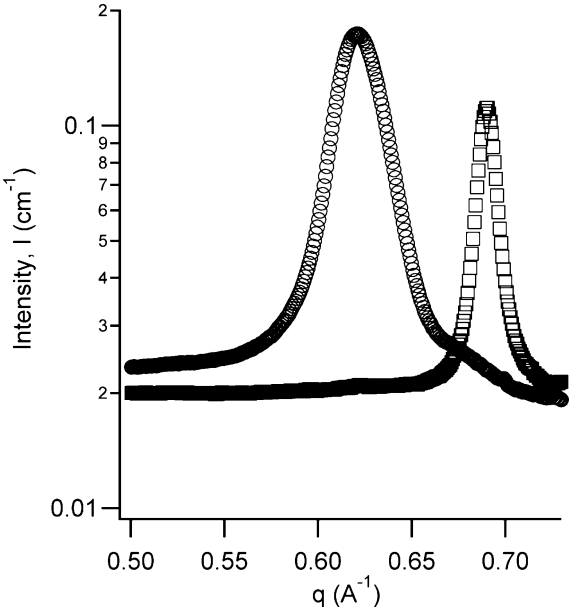

Figure 4. SAXS intensity profiles for poly(CPH:SA) (20:80) (○) and poly(CPH:SA) (80:20) (□).

Table 2. Number-Average Sequence Lengths Computed from ^{1}H NMR and the Calculated Radius of Gyration for the Longer Blocklike Sequence for the Copolymers Used in This Study

polymer	L_{CPH}	L_{SA}	$R_{g,1}$ (Å)	nl_2 (Å)
poly(CPH:SA) (20:80)	2.3	12.0	15.1	24.6
poly(CPH:SA) (80:20)	10.4	1.7	22.7	15.1

of these polymers. Thus, we cannot attribute this peak to a long period in the microphase separation. Rather, we associate these peaks with a dispersed phase that has a very uniform length scale, but no long-range periodic correlations. This interpretation is confirmed by comparing the domain sizes obtained from the solid-state NMR experiments to those obtained from the SAXS experiments (Table 1).

We interpret the significance of these results by comparison to calculations of random coil chain conformations. Table 2 shows the number-average sequence lengths obtained from solution state NMR and reported previously and the radius of gyration of the longer blocklike sequence, R_g.

$$R_g = \left(\frac{C_\infty n l^2}{6}\right)^{0.5} \tag{4}$$

Here, C_∞ is the characteristic ratio, n is the number of bonds in the blocklike sequence, and l is the average bond length. We have previously estimated the characteristic ratios for poly(CPH) and poly(SA) as 6.8 and 4.8, respectively, from molecular dynamics simulations.[13] The values of nl^2/mer for poly(CPH) and poly(SA) (where the mer units are defined by the structures in Figure 1) were obtained in the same studies as 43.7 and 23.8 Å^2, respectively. The radius of gyration of a block can be used to estimate the size of a domain of the majority component. For the minority component, the random coil approximation is not valid because of the relatively small number of bonds, so an estimate of the length scale associated with the minority component can be obtained by considering the contour length of a monomer, nl. Figure 5 is a schematic of our molecular description of the microphase separation in these weakly segregated blocklike copolymers.

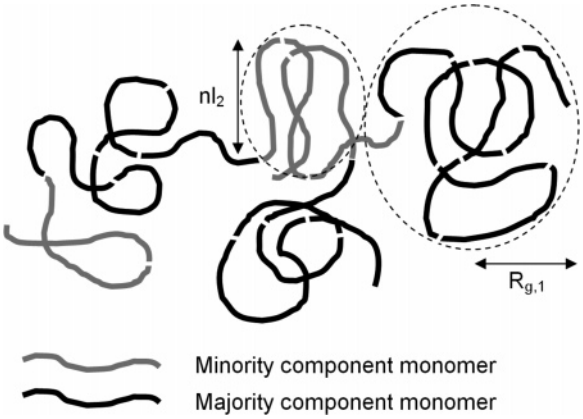

Figure 5. Schematic of microphase separation in a weakly segregated blocklike copolymer. The dimensions of the microphase-separated domains can be approximated by the radius of gyration for the majority component, $R_{g,1}$ (black), and the monomer contour length for the minority phase, nl_2 (gray).

These computed radii of gyration are on the same order of magnitude as the domain sizes computed from the solid-state NMR and the SAXS (Table 1). The simple random coil model used here to estimate the domain sizes does not account for such effects as an interphase thickness or enthalpic effects that force the two phases to separate and may put further restrictions on chain conformations. Because of these approximations, the domain sizes are slightly overestimated by the random coil calculations. However, these data support our hypothesis of a weakly segregated blocklike nanostructure in these copolymers. The structure results from the blocklike nature of the random copolymers coupled with the propensity of these materials to phase separate. Comparing the radii of gyration approximated from the random coil approximation to the domain sizes computed from SAXS and solid-state NMR, we are led to the conclusion that in the bulk polymer the blocks of CPH and SA can segregate to form the nanostructure without conformational entropic penalties. This work shows, for the first time, the nanometer length scale of the weakly segregated domains, directly measured and independently confirmed by two methods.

A detailed knowledge of the length scale of microphase separation in these copolymers is important for rational design of drug delivery vehicles based on these polymers. This is because when small molecular weight drug molecules are loaded into these copolymers, they will attempt to distribute themselves into compatible regions until saturation is reached. Knowing the length scale of the domains will enable rational choice of the drug loading if the drug solubility in the polymer is known. If the solubility limit is exceeded, the drug will be forced to disperse itself into less compatible regions, leading to a pronounced burst effect. Thus, drug release profiles can be accurately programmed with a detailed knowledge of the polymer microstructure. Another important aspect of interest is that the use of microphase-separated polymers permits the incorporation of multiple drugs into the same device. This concept has important implications for rational design of vaccine delivery systems.

Conclusions

The solid-state NMR and SAXS experiments offer nanoscale resolution of the microphase separation in weakly segregated blocklike polyanhydride copolymers. These concentration fluctuations are characterized by length scales smaller than 25 Å. On the basis of the relatively large sizes of the monomers in these polymers, we conclude that the microphase-separated domains contain very few monomers and may be formed from a single block or a small number of blocks. This knowledge of the copolymer microstructure, coupled with accurate erosion and drug release models, will help guide the rational design of these materials for drug delivery as we pursue the synthesis of polyanhydride block copolymers.

Acknowledgment. We thank the Whitaker Foundation for financial support. This work benefited from the use of BESSRC-CAT at APS and IPNS, funded by the U.S. DOE, BES under Contract W-31-109-ENG-38 to the University of Chicago.

References and Notes

(1) Goepferich, A.; Alonso, M. J.; Langer, R. *Pharm. Res.* **1994**, *11*, 1568−1574.
(2) Leong, K. W.; Brott, B. C.; Langer, R. *J. Biomed. Mater. Res.* **1985**, *19*, 941−955.
(3) Mathiowitz, E.; Saltzman, W. M.; Domb, A.; Dor, Ph.; Langer, R. *J. Appl. Polym. Sci.* **1988**, *35*, 755−774.
(4) Mathiowitz, E.; Langer, R. *J. Controlled Release* **1987**, *5*, 13−22.
(5) Tabata, Y.; Domb, A.; Langer, R. *J. Pham. Sci.* **1994**, *83*, 5−11.
(6) Narasimhan, B.; Kipper, M. J. *Adv. Chem. Eng.* **2004**, *29*, 169−218.
(7) Shen, E.; Kipper, M. J.; Dziadul, B.; Lim, M.-K.; Narasimhan, B. *J. Controlled Release* **2002**, *82*, 115−125.
(8) Shen, E.; Pizsczek, R.; Dziadul, B.; Narasimhan, B. *Biomaterials* **2001**, *22*, 201−210.
(9) Shen, E. E.; Chen, H.-L.; Narasimhan, B. *Proc. Mater. Res. Soc.* **2001**, *662*, N.N.4.2.1−N.N.4.2.5.
(10) Kipper, M. J.; Narasimhan, B. *Macromolecules* **2005**, *38*, 1989−1999.
(11) Larobina, D.; Kipper, M. J.; Mensitieri, G.; Narasimhan, B. *AIChE J.* **2002**, *48*, 2960−2970.
(12) Kipper, M. J.; Seifert, S.; Thiyagarajan, P.; Narasimhan, B. *J. Polym. Sci., Part B: Polym. Phys.* **2005**, *43*, 463−477.
(13) Kipper, M. J.; Seifert, S.; Thiyagarajan, P.; Narasimhan, B. *Polymer* **2004**, *45*, 3329−3340.
(14) Ron, E.; Mathiowitz, E.; Mathiowitz, G.; Domb, A.; Langer, R. *Macromolecules* **1991**, *24*, 2278−2282.
(15) Heatley, F.; Humadi, M.; Law, R. V.; D'Emanuele, A. *Macromolecules* **1998**, *31*, 3832−3838.
(16) McCann, D. L.; Heatley, F.; D'Emanuele, A. *Polymer* **1999**, *40*, 2151−2162.
(17) Schmidt-Rohr, K.; Mao, J. D. *J. Am. Chem. Soc.* **2002**, *124*, 13938−13948.
(18) Clauss, J.; Schmidt-Rohr, K.; Spiess, H. W. *Acta Polym.* **1993**, *44*, 1−17.
(19) Schmidt-Rohr, K.; Spiess, H. W. *Multidimensional Solid-State NMR and Polymers*; Academic Press: San Diego, 1994.
(20) Seifert, S.; Winans, R. E.; Tiede, D. M.; Thiyagarajan, P. *J. Appl. Crystallogr.* **2000**, *33*, 782−784.
(21) Chen, Q.; Schmidt-Rohr, K. *Solid State NMR*, in press.

MA051267R